Programmable optical delay generator with uniform output and double-delay capability

L.-S. Yan, L. Lin, A. Belisle, S. Wey, and X. Steve Yao

General Photonics Corporation, 5228 Edison Avenue, Chino, California 91710, USA
lsyan@generalphotonics.com

Received June 28, 2006; revised October 23, 2006; accepted October 31, 2006; published December 13, 2006 (Doc. ID 72385)

We demonstrate a programmable optical delay generation scheme incorporating both single- and double-pass configurations. The generator uses fiber coils with binary lengths separated by microelectro mechanical systems (MEMS)-based optical switches and can provide a delay range of up to 80 and 160 μs for single- and double-pass configurations, respectively, with corresponding resolutions of ~39 and 78 ns. The response time of the delay generation is <1 ms with an output power variation of <0.3 dB as the delay varies. The described approach can be applied to packet-switching optical networks, microwave photonic networks, and measurement systems. © 2006 Optical Society of America

OCIS codes: 060.2360, 060.4250.

1. Introduction

Programmable time-delay lines with ranges from nanoseconds to milliseconds are key elements in various applications, such as optical networking functions (buffering, dispersion management, slowing light, encoder–decoders, etc.), rf systems (radar, wireless communication, rf link emulation, cell site characterization, and calibration, etc.), as well as measurement systems (laser linewidth, phase noise, etc.) [1–10]. Various configurations have been proposed and demonstrated to generate tunable time delays, including fiber coils [11,12], fiber Bragg gratings [8–13], integrated waveguide techniques [14,15], fiber loops [2], microelectro mechanical systems (MEMS)-switch-based configurations [16–18], and other methods [19,20]. Most of the generated delays (except fiber-coil-based ones) are limited to a range of picoseconds to nanoseconds. On the other hand, the fiber-coil-based time-delay approach is an old concept and has been demonstrated using either the square-root cascaded delay line configuration (SRODEL) [11] or the binary delay line configuration (BIFODEL) [12]. The BIFODEL architecture is the optimum choice for implementation of delay-compressive delay lines [7].

In this paper, we demonstrate a BIFODEL-architecture-based programmable optical delay generation scheme incorporating both single- and double-pass configurations. The generator uses fiber coils with binary lengths separated by MEMs-based optical switches and can provide a delay range of up to 80 and 160 μs for single- and double-pass configurations with corresponding resolutions of ~39 and 78 ns. The response time of the delay generation is <1 ms with an output power variation of <0.3 dB as the delay varies. The double-path configuration has the advantages of polarization-independent (i.e., polarization maintaining with single-mode fiber) and saving fiber coils for less space (size) requirements. Furthermore, we also discuss the applications of such approach into packet-switching optical networks, microwave photonic networks, and measurement systems.

2. Concept and Setup

The ODG setup is shown in Fig. 1. Twelve MEMS-based 2×2 optical switches are cascaded and controlled by a microprocessor. For each optical switch (except the last one), one output is directly connected to the input of the following switch, while the other output is connected through an optical fiber delay coil manufactured from standard

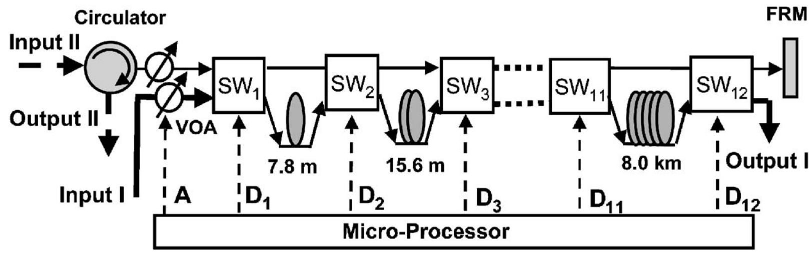

Fig. 1. Configuration of the programmable delay generator (ODG), single-pass (input I and output I) and double-pass (input II and output II); SW_i, MEMs-based optical switches; FRM, Faraday rotator mirror; VOA, Variable optical attenuator.

single-mode fiber (SMF). The lengths of the fiber coils are designed in a binary order from ~7.8 m (corresponding to ~39 ns delay) to ~8.0 km; thus, the total generated optical delay T_{total} is given by

$$T_{\text{total}} = \Delta T \sum_{n=1}^{N} [1-(-1)^{d_n}]2^{n-2}, \tag{1}$$

where ΔT is the delay of the minimum length coil (7.8 m), N is the total number of switches, and $d_n(=0,1)$ is the binary value of the nth switch condition, which determines whether or not the fiber coil following the nth optical switch is incorporated into the optical path.

To enhance the delay generation capability without complicated hardware modification, we simply incorporate an optical circulator and a Faraday rotator mirror (FRM) into the setup to create a double-pass configuration. This approach can significantly reduce the required package space of the delay line without adding another switch and a much longer delay coil (two times longer of the most significant coil). The result is two possible modes of operation: (i) For single-pass delay generation, light enters from one input port of the first switch and passes through all of the other switches and/or fiber coils, then exits from one output port of the last switch. (ii) Alternatively, light can be input from the first port of the circulator, which connects to the other input port of the first switch, then go through the other 11 switches and/or coils. After output from the last optical switch, the light is reflected at the FRM, passes back through the same optical path, and finally exits from the third port of the circulator. This configuration doubles the generated optical delay using the corresponding logic control.

Using the single- and double-pass configurations described above, delay ranges of up to 80 (corresponding to ~16 km SMF) and 160 μs are achieved. Note that the FRM in the setup provides the additional advantage of eliminating polarization-dependent effects along the optical path. The state of polarization (SOP) is maintained for the input and output light without the use of PM fiber; therefore, the delay generator can provide a low-cost solution for applications that require stable polarization. In addition, variable optical attenuators (VOA) are used to dynamically tune the insertion loss at different delay states, allowing the output power to remain relatively constant during delay switching.

3. Experimental Results

Insertion loss is one of the key parameters for programmable delay lines. Its variation with changes in delay is of particular interest. Figure 2 illustrates the insertion loss variation of the delay generator with delay and wavelength change. Figures 2(a) and 2(b) show the loss variation with delay change at 1550 nm for the single-pass case. Before the output power balancing using the VOA, the output power changes a lot at different delays. The typical loss ranges from ~3.4 to 8.5 dB including both the fiber coils and switches [Fig. 2(a)]. In our design, the VOA is automatically controlled by the microprocessor, using a look-up table to balance the output power at different logic states (delays). Therefore, the loss variation is limited to <0.3 dB over all delay states [Fig. 2(b)]. This feature ensures a stable performance for the applications that are sensitive to optical-signal-to-noise ratio (OSNR). Figure 2(c) shows the insertion loss profile of our delay generator over different wavelengths at a single switching condi-

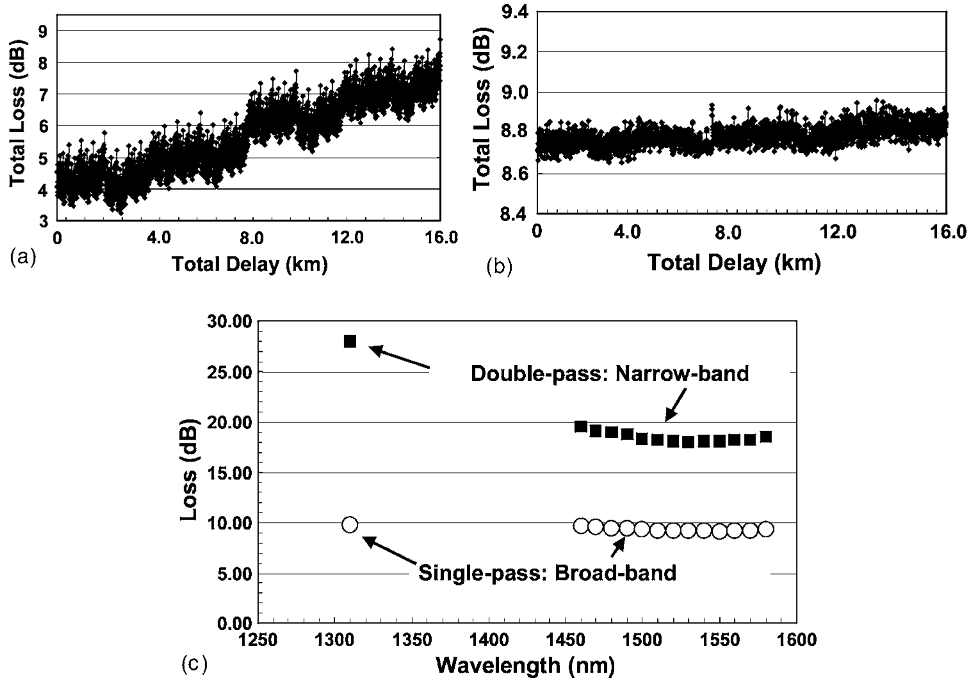

Fig. 2. (a), (b) Insertion loss variation at different delay settings (2048 logic states for the single-pass configuration at 1550 nm): (a) without automatic power balancing (b) using the VOA to automatically control the overall loss, thus the total variation <0.3 dB. (c) Insertion loss variations of the ODG at different wavelengths (single pass at 40 μs and double pass at 80 μs).

tion (40 and 80 μs delay for single- and double-pass. At 1550 nm, the typical insertion losses for single and double passes are ~9.1 and 18.5 dB with the VOA's automatic balancing. Since the optical switches are broadband devices (>400 nm), the insertion loss variation in the single-pass configuration is mainly due to the fiber coil itself (the range of wavelengths measured is limited by the experimental setup). However, there are two narrowband devices in the double-pass configuration: the optical circulator and the FRM; thus, the insertion loss of the double-pass configuration is much higher than twice that of the single-pass configuration at 1310 nm. The insertion loss of the single- and double-pass configurations at 1310 nm are ~10.0 and 28.4 dB, respectively. Note that the loss variation at different wavelengths is not necessary to be corrected using VOA due to the extremely high loss at certain wavelengths.

As mentioned, incorporating the FRM into the double-path configuration has another advantage, i.e., reducing the polarization-dependent effects, which is a desirable feature for some field applications (e.g., airborne systems). This is shown in Fig. 3(a), where the output polarization state keeps stable on the Poincaré sphere even under strong polarization perturbation on the delay line. Moreover, a fast response time is also required for dynamic applications. The delay generation speed of

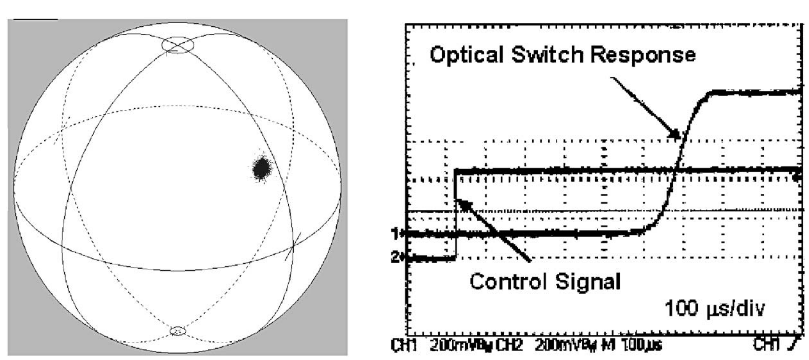

Fig. 3. (a) Polarization stability of the double-path configuration with external polarization perturbation; (b) measurement result of the response time for the ODG: <1 ms (~700 μs).

the ODG was characterized by measuring the transient traces from one delay to another, as shown in Fig. 3(b). The control signal is the electronic signal from the microprocessor, while the optical switch response is measured using a fast photodetector. If all 12 switches respond simultaneously (in parallel), the total response time is $<700\ \mu s$, suitable for most applications.

4. Applications

As mentioned in Section 1, the programmable optical delay generator can generate a series of digitized delay values for various applications, while it cannot provide continuous tuning for some special applications. In addition, the resolution of the ODG is limited by the "ability to manufacture" the minimum optical fiber length for fusion splicing (typically several tens of centimeters, with corresponding delays of hundreds of picoseconds), which may also be inadequate in some application. The demonstrated ODG can find its applications in the following areas:

(i) Optical networking functions: Due to the dynamic nature of optical packet-switching networks, programmable optical delay lines are essential for applications [1–4] such as optical buffering, temporal encoding to decoding, or even the management of optical dispersive effects. Buffers with tunable size are desirable to handle different packet sizes or variable bit rate (VBR) for optical networks (Fig. 4). Compared with previous looplike configurations, the ODG approach has the advantages of easier control and higher resolution. In addition, network carriers or equipment manufactures may use the ODG as an environmental emulator to evaluate the performance of the equipment or the system tolerance assuming data traffic from different nodes.

(ii) Microwave photonic networks: Optical delay lines have many applications for microwave photonic networks, such as phased-array antenna systems, optical wireless networks, signal processing (transversal filters), wireless (radar) ranging and calibration, and so on. Fixed delay arrays are used for some applications, while programmable delay lines are valuable to calibration procedures of wireless (cell) stations. An illustration of such an application is shown in Fig. 5. The wireless signal is separated into two paths: one is transmitted normally through the air and received by a wireless receiver, while another path is first converted into an optical signal using electro-optic modulator, and then transmitted through the programmable ODG. After ODG, the signal is converted back to the rf signal through optical-to-electronic conversion. The two rf signals will be combined and analyzed; therefore the ranging, noise, and related information of the wireless signal can be retrieved.

(iii) Measurement systems: Fiber delay lines are also very useful for some measurement systems, especially the linewidth of a laser source, phase noise, and so on. Figure 6 shows a typical diagram of a delayed self-heterodyne method to measure the linewidth of a laser source. It is an interferometric technique that incorporates a certain length of fiber delay coil in one arm. The superimposed beams from two arms are detected through a photodetector and thus analyzed using a spectrum analyzer. If the time delay is larger than the coherence length of the laser (normally at least five times longer is recommended for measurements), the phases of two beams are essen-

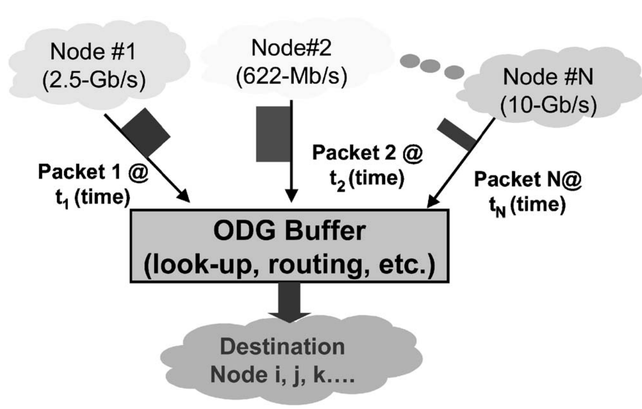

Fig. 4. Using ODG as a tunable optical buffer for a dynamic packet-switching network.

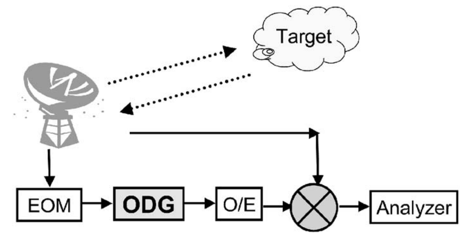

Fig. 5. Illustration of a rf ranging or calibration system utilizing the ODG platform. EOM, electro-optic modulator.

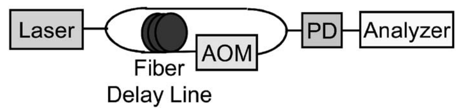

Fig. 6. Diagram of a delayed self-heterodyne measurement of a laser linewidth.

tially uncorrelated. Therefore the final output spectrum is a simple self-convolution of the spectrum of the laser itself, from which the linewidth can be readily obtained. As examples, a tunable laser with 50 kHz linewidth has a coherence length ~1.9 km, while the coherence length of a regular distributed feedback (DFB) laser with 50 MHz linewidth is approximately 190 m. Due to the variety of current available laser sources (Tunable, DFB, feedback positive, etc.), and the corresponding linewidth ranges from tens of kilohertz to gigahertz, a tunable (or programmable) optical delay generator certainly will facilitate such measurements.

5. Conclusions

The single- and double-path configurations of the above-demonstrated optical delay generator provide programmable optical delays with uniform output power, which is desirable for most of the applications. Advantages also include fast response time, large number of control bits, and high resolution. The potential delay range up to 0.25 ms with the same package size is under design and evaluation using the similar approach. When incorporating delay lines with more precise tuning resolutions [21], a widely and fully tunable delay generation is possible for various applications.

References

1. Y.-K. Yeo, J. Yu, and G.-K. Chang, “A dynamically reconfigurable folded-path time delay buffer for optical packet switching,” IEEE Photon. Technol. Lett. **16**, 2559–2561 (2004).
2. R. Langenhorst, M. Eiselt, W. Pieper, G. Grosskopf, R. Ludwig, L. Kuller, E. Dietrich, and H. G. Weber, “Fiber loop optical buffer,” J. Lightwave Technol. **14**, 324–335 (1996).
3. T. J. Eom, S. J. Kim, T.-Y. Kim, C.-S. Park, U.-C. Paek, and B. H. Lee, “Realization of true-time-delay using cascaded long-period fiber gratings: theory and applications to the optical pulse multiplication and temporal encoder/decoder,” J. Lightwave Technol. **23**, 597–608 (2005).
4. R. Geldenhuys, Z. Wang, N. Chi, I. Tafur Monroy, A. M. J. Koonen, H. J. S. Dorren, F. W. Leuschner, G. D. Khoe, and S. Yu, “Multiple recirculations through crosspoint switch fabric for recirculating optical buffering,” Electron. Lett. **41**, (2005).
5. J. Mora, B. Ortega, A. Di’ez, M. V. Andrés, J. Capmany, J. L. Cruz, and D. Pastor, “Highly tunable optically switched time delay line for transversal filtering,” Electron. Lett. **39**, 1799–1800 (2003).
6. T. Duthel, S. L. Jansen, M. Otto, P. M. Krummrich, and C. G. Schaffer, “Tunable all-fiber delay line filter for residual dispersion compensation in 40-Gbit/s systems,” Electron. Lett. **40**, 1291–1292 (2004).
7. A. P. Goutzoulis and D. K. Davies, “Hardware compressive 2-D fiber optic delay line architecture for time steering of phased array antennas,” Appl. Opt. **29**, 5353–5359 (1990).
8. J. L. Corral, J. Marti, S. Regidor, J. M. Foster, R. Laming, and M. J. Cole, “Continuously variable true time-delay optical feeder for phased-array antenna employing chirped fiber grating,” IEEE Trans. Microwave Theory Tech. **45**, 1531–1536 (1997).
9. H. Tsuchida, “Simple technique for improving the resolution of the delayed self-heterodyne method,” Opt. Lett. **15**, 640–642 (1990).
10. O. Raz, R. Rotman, and M. Tur, “Wavelength-controlled photonic true time delay for wide-band applications,” IEEE Photon. Technol. Lett. **17**, 1076–1078 (2005).
11. R. A. Soref, “Programmable time-delay devices,” Appl. Opt. **23**, 3736–3737 (1984).
12. A. P. Goutzoulis, D. K. Davies, and J. M. Zomp, “Prototype binary fiber optic delay line,” Opt. Eng. (Bellingham) **28**, 1193–1202 (1989).

13. V. Italia, M. Pisco, S. Campopiano, A. Cusano, and A. Cutolo, “Chirped fiber Bragg gratings for electrically tunable time delay lines,” IEEE J. Sel. Top. Quantum Electron. **11**, 408–416 (2005).
14. B. Vidal, J. L. Corral, and J. Marti, “Optical delay line employing an arrayed waveguide grating in fold-back configuration,” IEEE Microw. Wirel. Compon. Lett. **13**, 238–240 (2003).
15. B. Howley, Y. Chen, X. Wang, Q. Zhou, Z. Shi, Y. Jiang, and R. T. Chen, “2-bit reconfigurable true time delay lines using 2×2 polymer waveguide switches,” IEEE Photon. Technol. Lett. **17**, 1944–1946 (2005).
16. J. D. Shin, Y. M. Yoon, B. M. Jung, and B.-G. Kim, “A 4-bit optical true time-delay for 10-GHz phased array antennas using optical MEMS switches and fiber-optical delay lines,” in *The 17th Annual Meeting of the IEEE Laser and Electro-Optics Society (LEOS)* (2004), Vol. 1, pp. 274–275.
17. J. D. Shin, B.-S. Lee, and B.-G. Kim, “Optical true time-delay feeder for X-band phased array antennas composed of 2×2 optical MEMS switches and fiber delay lines,” IEEE Photon. Technol. Lett. **16**, 1364–1366 (2004).
18. V. Kaman, X. Zheng, R. J. Helkey, C. Pusarla, and J. E. Bowers, “A 32-element 8-bit photonic true-time-delay system based on a 288×288 3-D MEMS optical switch,” IEEE Photon. Technol. Lett. **15**, 849–851 (2003).
19. P. Maak, I. Frigyes, L. Jakab, I. Habermayer, M. Gyukics, and P. Richter, “Realization of true-time delay lines based on acoustooptics,” J. Lightwave Technol. **20**, 730–739 (2002).
20. O. Raz, R. Rotman, Y. Danziger, and M. Tur, “Implementation of photonic true time delay using high-order-mode dispersion compensating fibers,” IEEE Photon. Technol. Lett. **16**, 1367–1369 (2004).
21. Data sheet of miniature motorized optical variable delay line MDL-002, Web site http://www.generalphotonics.com/MiniMDL.htm.